ACCURATELY MEASURING UNSTEADY WATER FLOWS USING A DYNAMIC STANDARD

I. I. Shinder and M. R. Moldover
Process Measurements Division, National Institute of Standards and Technology, Gathersburg, MD 20899-8360, USA

Abstract - We recently presented and tested a model for a dynamic gravimetric standard for steady water flows. In the range 10 kg/s to 60 kg/s, the difference between the dynamic standard and NIST's static primary standard was 0.015 % with a standard deviation of 0.033 %, Here, we extend the model for the dynamic gravimetric standard to account for unsteady flows and we account for the different response times of the dynamic standard and an electromagnetic flow meter (EMF). After these improvements, we measured water flows with diverse time dependences during 100 s collection intervals. These flows averaged 12 kg/s; however, the flows ramped or stepped up or down 5 kg/s. When integrated over the collection interval, the difference between the dynamic standard and a statically-calibrated EMF was 0.008 % with a standard deviation of 0.012 %. This agreement justifies the further study of the dynamic standard, particularly at higher flows where the mechanical simplicity of a dynamic standard might reduce the cost of accurate measurements.

INTRODUCTION

The present research is motivated by the need to extend NIST's calibration services for water flow meters to higher flows at moderate cost. At present, NIST's water flow calibration facility (WFCF) determines the average mass flow rate $\langle \dot{m} \rangle$ from two static weighings and a measured time interval. The collection tank is weighed just before the steady water flow is diverted from a bypass into the tank, and the tank is weighed again just after the water flow is diverted from the collection tank back into the bypass. (See Fig.1.) The WFCF achieves a standard relative uncertainty of 0.016 % < $u_r(\dot{m})$ < 0.026 % for mass flows in the range 0.7 kg/s to 60 kg/s [1]. These low uncertainties are achieved, in part, because the WFCF uses a carefully engineered collector/bypass (C/B) unit that reduced the standard uncertainty of the the measured collection time interval to less than 2.5 ms. (The C/B unit is a uni-directional diverter that always travels in the same direction when it cuts the flow.) However, at flows above 60 kg/s, water splashes out of the diverter and greatly increases the uncertainty of calibrations. To avoid the expense of building a larger uni-directional diverter, we investigated the dynamic method.

The dynamic standard used the same WFCF hardware; however the weight W was recorded every 49.1517 ms while the water flow filled the collection tank. The stream of weighing data was analyzed to compute the average derivative $\langle dW/dt \rangle$, from which $\langle \dot{m} \rangle$ was determined. The interval for the averages was defined by the electronics of the weigh scale and the computer that recorded the weighings. The simplicity of the dynamic timing is advantageous for measuring much larger flows than we consider here.

In a recent publication [2], we tested the dynamic approach using constant flows in the range 10 kg/s < $\dot{m}$ < 60 kg/s. Because the flows were constant, we ignored the transient responses of the dynamic weighing system and of the electromagnetic flow meter (EMF) used in the tests, and we used a simplified model to relate the mass flow $\dot{m}$ to the time derivative of the weight dW/dt. Despite these simplifications, the difference between the dynamic standard and NIST's static primary standard was 0.015 % $\pm$ 0.033 %, in the range 10 kg/s to 60 kg/s.

In this work, we extend our study of the feasibility of dynamically measuring $\dot{m}$ by accounting for the response times of the instruments and the dynamic standard and by using an improved model. We tested these improvements using flows that averaged 12 kg/s but were either ramped or stepped up or down such that the flow changed 5 kg/s during a significant portion of a 100 second long collection interval. When integrated over the collection interval, the fractional difference between the dynamic standard and a statically-calibrated electromagnetic flow meter (EMF) was 0.008 % and the standard deviation the measurements was 0.012 % This standard deviation is only slightly larger than 0.009 %, the standard deviation of the calibration data for the EMF. Thus, the dynamic and static standards agree within the uncertainty of this comparison. This agreement justifies the further study of the dynamic standard, particularly at higher flows where the mechanical simplicity of a dynamic standard might reduce the cost of accurate measurements.

The remainder of this report is organized as follows. We describe the apparatus used in this research (WFCF) and we review the results obtained for the dynamic standard using steady flows. Then, we model the dynamic standard and derive the expression used to deduce $\langle \dot{m} \rangle$ from $W(t)$, the time-dependent readings of the weigh scale. Because we used an EMF to test the dynamic standard, we discuss the static calibrations of this meter. Finally, we describe the new tests of the dynamic standard using varying flows.

WATER FLOW CALIBRATON FACILITY

This research was conducted using NIST's water-flow calibration facility (WFCF) that is sketched in Figure 1. Details concerning the WFCF are provided in [1] and [2]. The WFCF uses the relation:

$$\dot{m} = \frac{W_{\mathrm{f}} - W_{\mathrm{i}}}{g\Delta t(1-\rho_{\mathrm{air}}/\rho_{\mathrm{water}})} + \frac{(\rho_{\mathrm{f}} - \rho_{\mathrm{i}})V_{\mathrm{inventory}}}{\Delta t} \qquad (1)$$

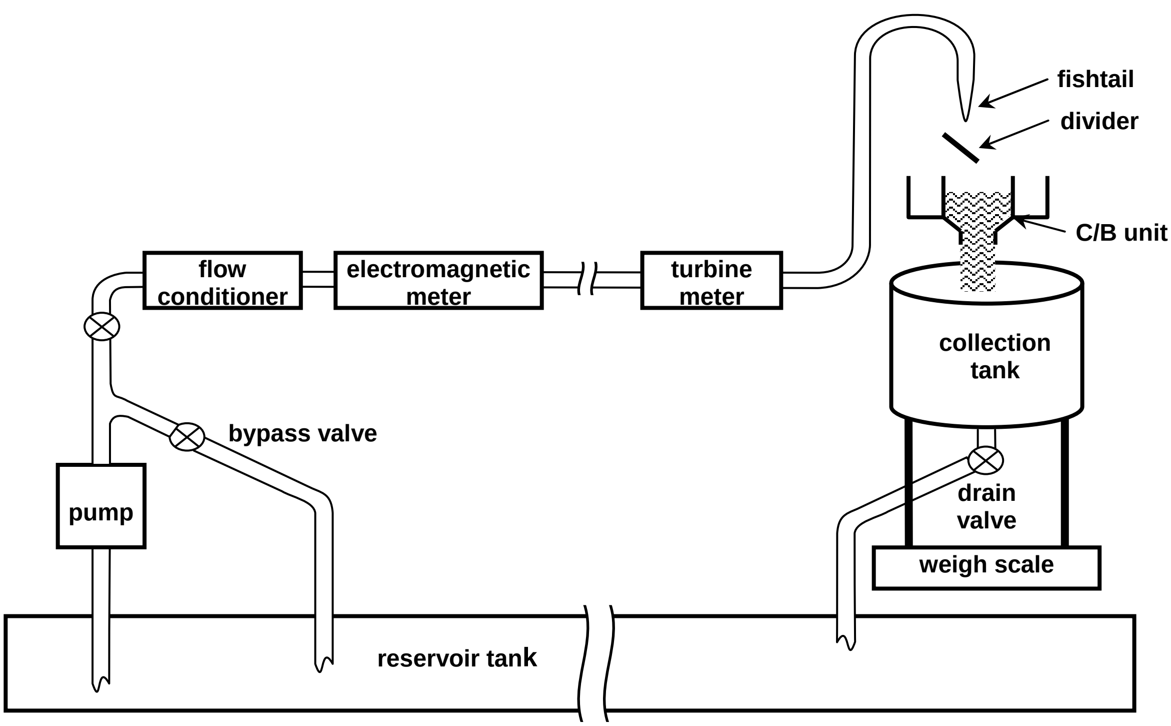

Figure 1. NIST's water flow calibration facility.

to determine the average mass flow $\dot{m}$ through the meter being calibrated. In Eq. (1), $\Delta W \equiv W_f - W_i$, is the change in the weight of the collection tank during the collection time interval $\Delta t \equiv t_f - t_i$, $V_{inventory}$ is the inventory volume, *i.e*. the volume piping between the meter under test and the end of the pipe used to measure the flow, ρ_i and ρ_f are the densities in the inventory volume at the beginning and the end of the collection interval, and the term $(1-\rho_{air}/\rho_{water})$ is a buoyancy correction. The WFCF achieves a relative standard uncertainty $0.016\ \% < u^r(\dot{m}) < 0.026\ \%$ for mass flows in the range 0.7 kg/s to 60 kg/s [1].

As in [2], we used the 10 cm diameter flow line of the WFCF. The flows, 10 kg/s to 60 kg/s, correspond to Reynolds' numbers of 130,000 to 800,000, referred to the pipe's diameter. For comparing static and dynamic flow measurements, the key components of the WFCF are the collector/bypass (C/B) unit, the collection tank, the weigh scale, and check standards. Here, we shall describe the weigh scale; the reader can learn details concerning the C/B unit, the collection tank, and the check standards in [2].

The collection tank was supported on a commercially manufactured weigh scale (Mettler-Toledo, Model 2255-0151)*. The scale has a capacity of 4500 kg and a resolution of 10 g. To calibrate the scale, we used a set of twelve 45 kg steel masses that are traceable to the kilogram through NIST's Mass and Force Group. Two methods were used to calibrate the scale over its full range. The first method is described in detail in [1]. For this method, the scale was read while it supported the empty collection tank. Then, the 12 masses (540 kg) were loaded onto the scale and it was read again. Then the masses were unloaded, approximately 540 kg of water was added to the collection tank, and the scale was read a third time. This sequence was repeated until the capacity of the scale was reached.

The second method of calibrating the scale used two commercially-manufactured water flow meters that had acceptable short-term stability (repeatability). The calibration factors for the flow meters were measured by flowing approximately 540 kg of water into the collection tank at a flow of 10 kg/s for a collection time of approximately 54 s. Then, these calibration factors were used with longer collection times to check the scale readings at intervals of approximately 500 kg. During these checks, the flow rate was maintained near 10 kg/s. Thus, this calibration relies on the short-term stability and linearity of the flow meters. The meters were a 100 mm electromagnetic flow meter (manufacturer: Krohne, model Optiflux 5000) and dual rotor flowmeter (100 mm ExactFlow). Both calibration methods produced the same result; the weigh scale readout was a linear function of the load with the calibration coefficient $K_{scale} = 0.998789 + 4.57\times10^{-5}(t/^\circ\mathrm{C} - 20.3)$. The standard uncertainty of K_{scale} was 0.005 %.

The weigh scale was used with a commercially-manufactured (Toledo-Mettler, model "Jagxtreme") signal-conditioning unit with digital outputs. For all the measurements reported here, the low-pass filter was set at 2 Hz. For dynamic flow calibrations, the weight on the scale must be determined at precisely defined intervals. This was accomplished by utilizing the continuous output of the signal-conditioning unit, synchronized with its internal clock. Every 49.1517 ms, the scale delivered a digital output that we recorded. In separate measurements, we verified that the weigh scale's clock was stable, fractionally to 5×10^{-6}.

* In order to describe materials and procedures adequately, it is occasionally necessary to identify commercial products by manufacturer's name or label. In no instance does such identification imply endorsement by the National Institute of Standards and Technology, nor does it imply that the particular product or equipment is necessarily the best available for the purpose.

MODEL FOR THE DYNAMIC FLOW STANDARD

Figure 2 displays a simplified model of our dynamic flow standard. The C/B unit collects water from the fishtail and funnels it into a jet. We assume the velocity of the jet is zero at the height $h = 0$ in the C/B unit. The jet falls a distance h attaining the velocity $V = (2gh_1)^{1/2}$ as it enters the water already in the collection tank. We assume that neither the water in the collection tank, the tank itself, nor the weigh scale can store significant vertical momentum for times that are comparable to the collection time. In other words, the vertical component of momentum in the jet $p = \dot{m}V$ is promptly delivered to the weigh scale. Under this assumption, an ideal weigh scale reads the sum of three terms, a tare, the weight of the collected water m, and the impulse delivered to the scale by the jet: $W = \text{tare} + mg + \dot{m}V$. For the remainder of this manuscript, we shall ignore the tare and absorb the buoyancy correction into an effective acceleration due to gravity that will be denoted $g_{\text{eff}} \equiv g\times(1-\rho_{\text{air}}/\rho_{\text{water}})$. During the interval $\Delta t \equiv (t_2 - t_1)$ the mass of water collected increases by $(m_2 - m_1)$. During the same time interval Δt, the mass of water that flowed through the upstream meters is $\Delta m \equiv (m_2 - m_1 - m_{\text{jet}})$, where m_{jet} is the mass of the jet between the heights h_2 and h_1.

The scale readings at the times t_1 and t_2 are:

$$\frac{W_1}{g_{\text{eff}}} = m_1 + \frac{\dot{m}V_1}{g_{\text{eff}}} \quad ; \qquad \frac{W_2}{g_{\text{eff}}} = m_2 + \frac{(\dot{m}+\Delta\dot{m})V_2}{g_{\text{eff}}} \quad , \tag{2}$$

where $\Delta\dot{m}$ is flow change during the time interval $\Delta t \equiv (t_2 - t_1)$. The second equation can be re-written:

$$\frac{W_2}{g_{\text{eff}}} = m_1 + m_{\text{jet}} + \Delta m + \frac{(\dot{m}+\Delta\dot{m})V_2}{g_{\text{eff}}} \tag{3}$$

Δm is the mass collected during Δt. From Eqs. (2) and (3) one can find

$$\Delta m = \frac{W_2}{g_{\text{eff}}} - \left(\frac{W_1}{g_{\text{eff}}} - \frac{\dot{m}V_1}{g_{\text{eff}}}\right) - m_{\text{jet}} - \frac{(\dot{m}+\Delta\dot{m})V_2}{g_{\text{eff}}} \tag{4}$$

or

$$\Delta m = \frac{W_2 - W_1}{g_{\text{eff}}} + \frac{\dot{m}V_1}{g_{\text{eff}}} - m_{\text{jet}} - \frac{(\dot{m}+\Delta\dot{m})V_2}{g_{\text{eff}}} \tag{5}$$

We assume that the jet's velocity changes only because it falls through the distance between the end of funnel and the surface of the water in the collection tank. Then, we re-write Eq. (5)

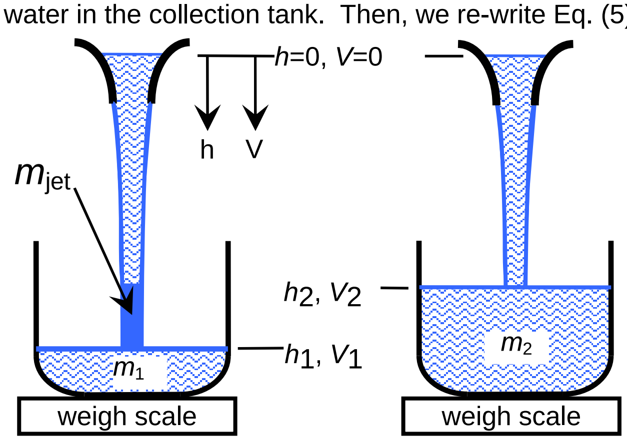

Figure 2. Schematic diagram of a dynamic calibration system at two times, t_1 and t_2.

$$\Delta m = \frac{W_2 - W_1}{g_{\text{eff}}} + \frac{\dot{m}V(h_1)}{g_{\text{eff}}} - m_{\text{jet}} - \frac{(\dot{m} + \Delta\dot{m})V(h_2)}{g_{\text{eff}}} \quad . \tag{6}$$

The mass of the water jet between levels 1 and 2 is:

$$m_{\text{jet}} = \dot{m}\tau = \dot{m}\left(\frac{V(h_1) - V(h_2)}{g_{\text{eff}}}\right) \quad , \tag{7}$$

where τ is time for a volume element in the jet to flow from level 2 to level 1. After substituting (7) into (6)

$$\Delta m = \frac{\Delta W}{g_{\text{eff}}} + \frac{\dot{m}V(h_1)}{g_{\text{eff}}} - \dot{m}\left(\frac{V(h_1) - V(h_2)}{g_{\text{eff}}}\right) - \frac{(\dot{m} + \Delta\dot{m})V(h_2)}{g_{\text{eff}}} \tag{8}$$

and simplifying, we obtain:

$$\Delta m = \frac{\Delta W}{g_{\text{eff}}} - \frac{\Delta\dot{m}V(h_2)}{g_{\text{eff}}} \quad , \tag{9}$$

or, in differential form

$$\dot{m} = \frac{\dot{W}}{g_{\text{eff}}} - \ddot{m}\frac{V(h)}{g_{\text{eff}}} \quad . \tag{10}$$

We omit subscript 2 for the jet velocity to generalize the equation. If $\dot{m}$ is constant, the last term is zero and we recover the simple model that was used in [2]:

$$\dot{m} = \dot{W}/g_{\text{eff}} \tag{11}$$

In this work, we used averages of Eq. (10) to compute the average flow during dynamic weighings. This equation will not be accurate if water flowing within the control volume has a time-dependent net component of vertical momentum. In [2] we argued that many flows in the collection tank do not have net vertical motions of the center of mass of the water; such flows cannot affect the readings of the weigh scale. However, the jet entering the collection tank generated bubbles that rose towards the water's surface, thereby allowing the center of mass of the water beneath the surface to fall; such flows have a net vertical component of momentum. We looked for a change in the water level immediately after the jet stopped and found none within a tolerance of 10 cm. This observation showed that the vertical component of momentum was negligible.

TESTS OF THE DYNAMIC STANDARD WITH STEADY FLOWS

In [2] we used the WFCF in two different ways simultaneously, thereby comparing NIST's static water flow standard with dynamic measurements. The comparison used steady flows and the simplified model, Equation (11). The results are displayed in Figure 3 and summarized by the observation that, during two runs 7 days apart and spanning the range 10 kg/s < $\dot{m}$ < 60 kg/s, the difference between the flow measured dynamically and averaged over the collection interval $\langle \dot{m}_{\text{D}} \rangle$ and the flow determined by NIST's static flow standard during the same interval $\dot{m}_{\text{S}}$ was 0.015 % with a standard deviation of 0.033 % of the flow. A concise way of expressing this result is: ($\langle \dot{m}_{\text{D}} \rangle / \dot{m}_{\text{S}} - 1$) = (1.5 ± 3.3) $\times 10^{-4}$.

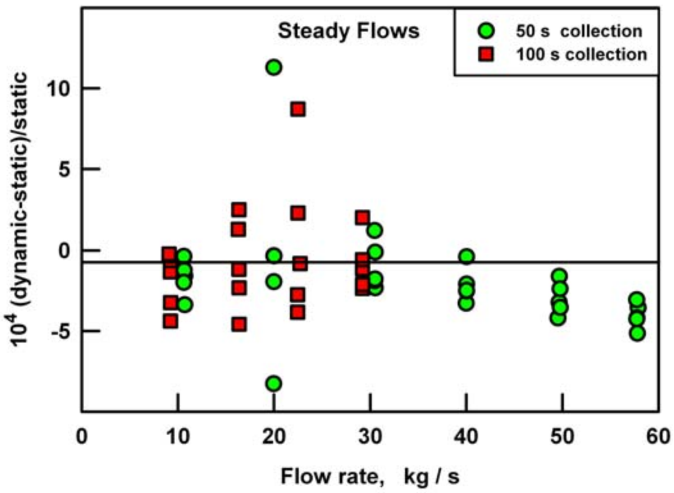

Figure 3. Fractional differences between dynamic measurements and NIST's static gravimetric standard for steady flows from [2].

Unexpectedly, the scatter in Fig. 3 depends on the flow; it has a maximum near 20 kg/s. We observed that the exit aperture of the fishtail (Fig. 1) is never completely filled for flows well below 20 kg/s and it is always completely filled for flows well above 20 kg/s. Near 20 kg/s, the flow randomly switches between filled and not-filled states, and the switching generates excess fluctuations in the flow. Nevertheless, the primary standard and the dynamic measurements agreed within the uncertainty of the comparison

TESTS OF THE DYNAMIC STANDARD WITH TIME DEPENDENT FLOWS

In order to test the dynamic standard with flows that vary in time, we required a well-characterized, stable, flow meter that responds rapidly to changing flows. For this purpose, we chose an electromagnetic flow meter (EMF). We calibrated the EMF using NIST's gravimetric static standard and then we compared the output of the EMF to the output from the dynamic standard as the flow varied.

Figure 4 displays the results of calibrating the EMF three times. All of the plotted data can be fit by a single linear function: K-factor = $0.996015 - 0.000054\times \dot{m}/(\mathrm{kg\ s^{-1}})$. The standard deviation of a single measurement from this function was 0.00009.

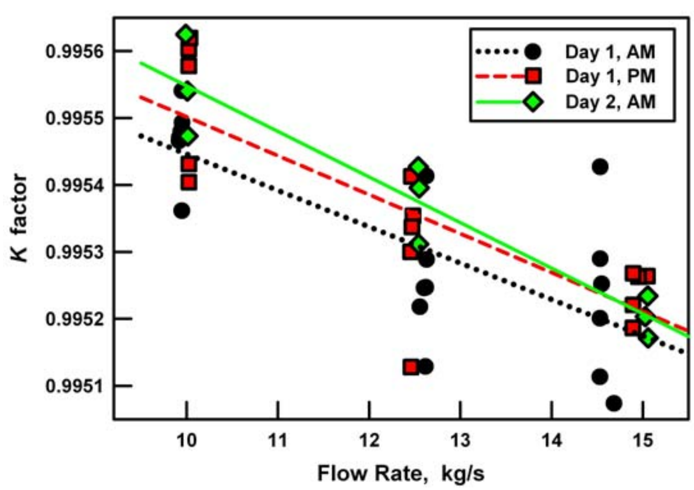

Figure 4. Calibration of electromagnetic flow meter.

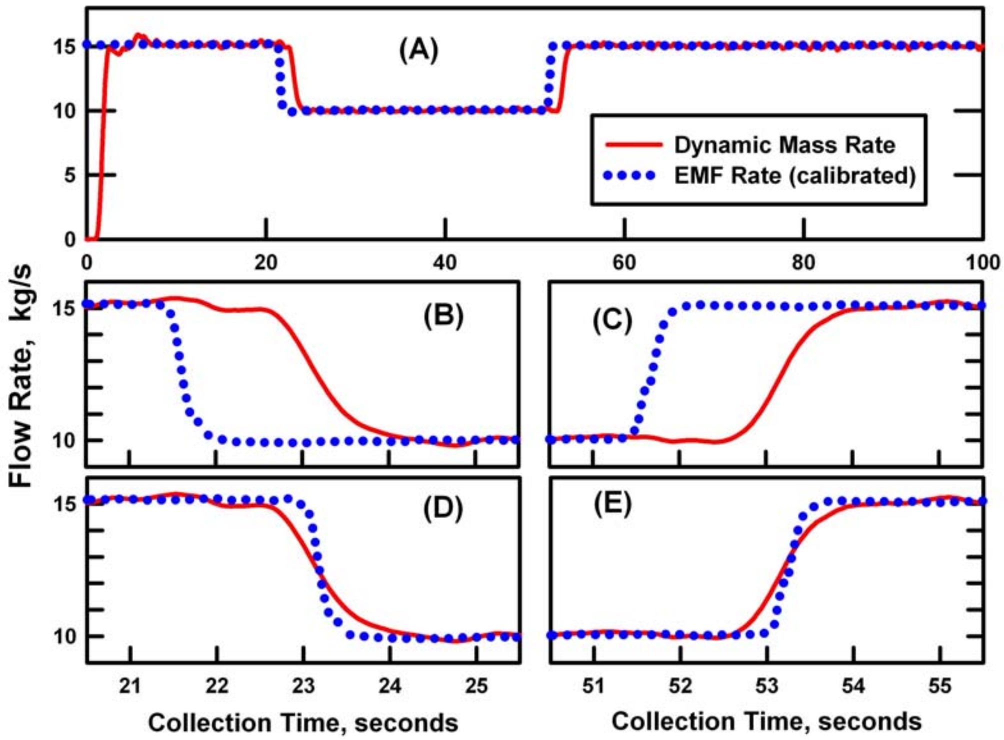

Figure 5. Flow deduced from the weigh scale data (dynamic mass rate) and from the electro-magnetic flow meter. In panels (D) and (E), the EMF data are plotted 1.57 s after the recorded time.

For variable flow measurements, it was essential to synchronize the data acquisition from the EMF and the dynamic system. Furthermore, it was necessary to measure how the EMF and the dynamic system responded to changes in flow. Figure 5 shows how this was done. Panel (A) displays the data recorded from the dynamic standard (weigh scale) and the EMF. At the start of this record, the 15 kg/s flow was switched from the bypass to the collection tank. At 21 seconds, the flow was reduced to 10 kg/s and at 51 seconds the flow was returned to 15 kg/s. (Below, we shall refer to this time-dependence as "pulse down.") Panels (B) and (C) of Fig. 5 are enlargements of a portion of Panel (A).

Panels (D) and (E) of Fig. 5 display the effects of adding a 1.57 s offset to the EMF time record. (1.57 s ≈ 32 time steps, each 49.1514 ms long) This offset was chose so that, the records from the weigh scale and the EMF coincide during both the middle of the step down and the step up of $\dot{m}$. The 1.57 s offset has at least five sources: (1) the transit time of the water from the EMF to the C/B unit, (2) the time the water is held within the C/B unit, (3) the time for the jet to fall from the C/B unit into the collection tank, (4) the mechanical and electronic responses of the weigh scale, and (5) the electronic response of the EMF. Crude estimates of these five sources are: (1) 0.3; (2) 0.2 s; (3) 0.5 s; (4) 0.7 s; (5) –0.2 s. [The minus sign in front of (5) indicates that (5) reduces the required offset.] In this work, we used a constant 1.57 s delay time, thereby, ignoring the weak dependencies of the delay time on $\dot{m}$ in terms (1), (2), and (3).

The weigh scale and the EMF deliver their output data in time-stamped streams. To analyze these data using Eq. (9), the model for the dynamic flow standard, we cast the equation into a difference form. The difference between two consecutive scale readings is:

$$\frac{W_{n+1} - W_n}{g_{eff}} = \frac{\dot{m}_n + \dot{m}_{n+1}}{2}\Delta t + \left(\dot{m}_{n+1} - \dot{m}_n\right)\sqrt{\frac{2h}{g_{eff}}} \quad , \tag{12}$$

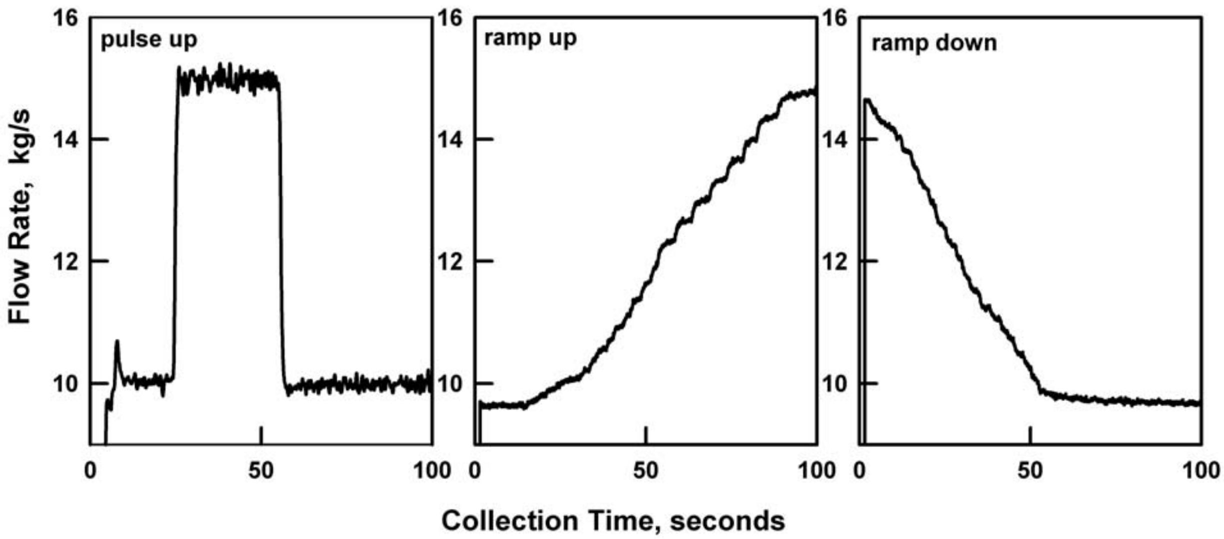

Figure 6. Calculated flows based on time dependent dynamic mass flow model (Eq. 14) for three of the four unsteady flows studied in this work.

where *h* is the height the jet falls from the reference (free) surface in the C/B unit into the collection tank. The reference surface in the C/B unit is 2.2 m above the bottom of the collection tank. When the cylindrical collection tank is filled to capacity (3000 kg) the water level is 1.3 m above the tank's bottom. Thus, *h* is calculated without free parameters from the expression:

$$h/\mathrm{m} = 2.2 - 1.3 M_\mathrm{n} /(3000\ \mathrm{kg}) \quad , \qquad (13)$$

and the mass flow can be found recursively at each time step:

$$\dot{m}_{\mathrm{n}+1} = \left[\frac{W_{\mathrm{n}+1} - W_\mathrm{n}}{g_\mathrm{eff}} - \dot{m}_\mathrm{n} \left(\frac{\Delta t}{2} - \sqrt{\frac{2h}{g_\mathrm{eff}}} \right) \right] \Bigg/ \left(\frac{\Delta t}{2} + \sqrt{\frac{2h}{g_\mathrm{eff}}} \right) \quad . \qquad (14)$$

We took data for four time dependent flows: the "pulse down" flow shown in Fig. 5 and the three flows shown in Fig. 6, which we call "pulse up", "ramp up", and "ramp down". For comparisons with these varying flows, we also analyzed data for several steady flows spanning the range 10 kg/s < $\dot{m}$ < 15 kg/s. Note: these data compare the dynamic mass flow with the EMF; thus, they differ from the earlier data plotted in Fig. 3 which compare the dynamic mass flow with NIST's static gravimetric standard.

RESULTS

The data were sorted into two groups: (1) steady flows, and (2) unsteady flows.(four cases including ramp up, ramp down, pulse up, pulse down). The analysis was conducted using two versions of the model: (1) variable flow, and (2) steady flow. The variable flow model uses Eqs. (12) – (14), which are numerical approximations to Eq. (9). The steady flow model assumes that *h* in Eq. (13) is zero; thus, it is equivalent to Eq. (10) and the model used in [2]. The results for the four cases are displayed in Figure 7.

Figure 7 shows that either the static or the dynamic model is satisfactory for steady flows. For steady flows, the tabulated values of the difference between the dynamic measurements and the EMF are comparable to the differences between successive calibrations of the EMF. Thus, dynamic gravimetric flow meter agrees with the calibrated EMF within the uncertainty of this comparison.

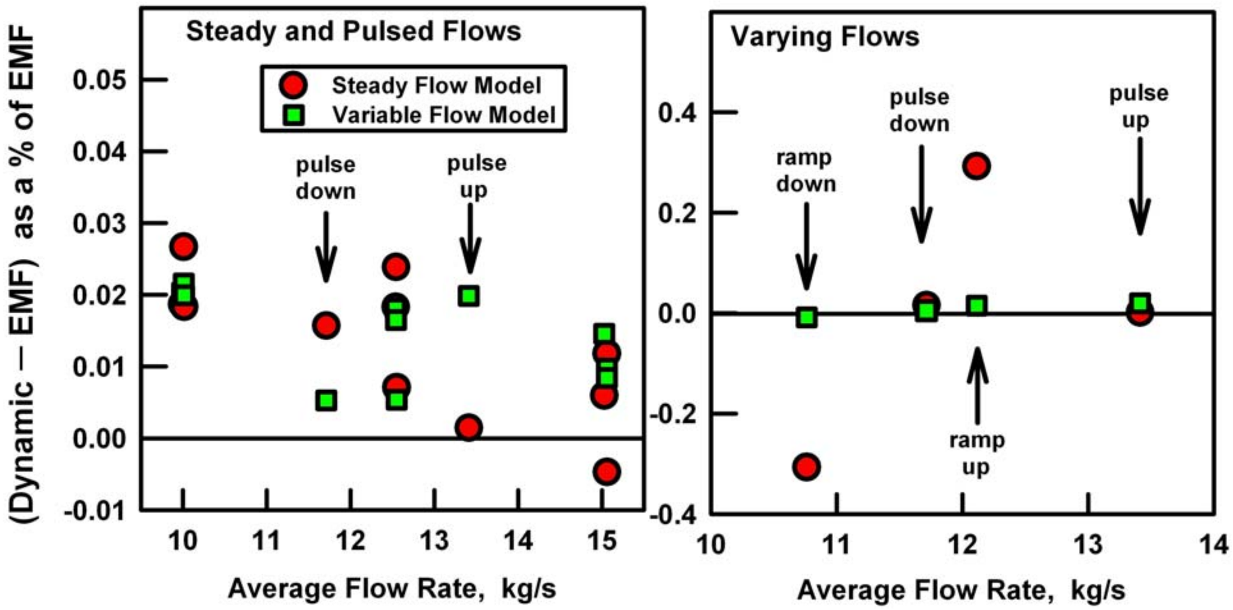

Figure 7. Comparisons of dynamic flow measurement and calibrated EMF. The variable flow model [Eq. (10)] was implemented numerically using Eqs. (12) - (14). For the steady flow model, $h \equiv 0$ in Eq. (13). Note: the scale on the left panel is 14× finer than the scale on the right panel.

In Figure 7, the results for the pulse flows resemble those for steady flows. This is expected after considering, for example, the step-down flow displayed in Fig. 5. For this flow, the $\ddot{m}$ term in Eq. (10) is zero except during two small parts of the collection interval: (1), near 21 seconds, when the flow steps down and (2) near 51 seconds, when the flow steps up. During the step-down, $\ddot{m}$ is negative and the contribution of the $\ddot{m}$ term to $\langle \dot{m} \rangle$ is positive. During the step-up, the signs are reversed. Thus, the step-up and step-down contributions tend to cancel; they do not cancel exactly because the water level in the collection tank is higher during the step-up than during the step-down. In contrast, there is no cancellation for the ramp flows. The average of the $\ddot{m}$ term in Eq. (10) contributes 0.3 % to $\langle \dot{m} \rangle$ during the ramp down; the sign is reversed during the ramp up.

To conclude, we emphasize that, when the variable flow model is used, the dynamic gravimetric flow meter agrees with the calibrated EMF for all the flows, within the uncertainty of the calibration of the EMF.

In the future, it would be desirable to test our assumption that the time delay between the dynamic flow meter and the EMF is independent of the flow over a wider range of flows. Of course, it would be desirable to test the dynamic flow meter at much larger flows.

REFERENCES

[1] Iosif I. Shinder, Iryna V. Marfenko. *NIST Calibration Services for Water Flowmeters. Water Flow Calibration Facility.* NIST Special Publication SP 250-73.
http://ts.nist.gov/MeasurementServices/Calibrations/upload/SP250_73.pdf

[2] Iosif I. Shinder and Michael R. Moldover. Feasibility of an Accurate Dynamic Standard for Water Flow, Flow Measurement and Instrumentation (submitted in 2008)